Improvement of satellite-to-ground QKD secret key rate with adaptive optics

Valentina Marulanda Acosta, Daniele Dequal, Matteo Schiavon, Aurélie Montmerle-Bonnefois, Caroline B. Lim, Jean-Marc Conan, Eleni Diamanti

Improvement of satellite-to-ground QKD secret key rate with adaptive optics

Valentina Marulanda Acosta,[1,2,*] Daniele Dequal,[3] Matteo Schiavon,[2] Aurélie Montmerle-Bonnefois,[1] Caroline B. Lim,[4] Jean-Marc Conan[1], and Eleni Diamanti[2]

[1] *DOTA, ONERA, Université Paris Saclay, F-92322 Châtillon, France*
[2] *Sorbonne Université, CNRS, LIP6, F-75005 Paris, France*
[3] *Telecommunication and Navigation Division, Agenzia Spaziale Italiana, Matera, Italy*
[4] *LNE-SYRTE, Observatoire de Paris, Université PSL, CNRS, Sorbonne Université, F-75014 Paris, France*

[*] *Valentina.Marulanda-Acosta@lip6.fr*

Abstract: We demonstrate the gain brought by adaptive optics for space-ground QKD links. Refined modeling of turbulence, adaptive optics and QKD, including finite-size effects, shows improvement by several orders of magnitude of the secret key rate.

1. Introduction

While QKD links enable security levels unattainable by classical means, their implementation on a global scale faces critical limitations due to optical fiber losses, which increase exponentially with distance. Without mature enough technology for quantum repeaters, the reachable distances of a terrestrial QKD setup are restricted to several hundred kilometers at most [1–3]. As a result, satellite relays have been projected as a very promising solution for the implementation of intercontinental links [4], with the publication of several theoretical and experimental feasibility studies about free-space satellite QKD over the years [5–11]. However, for satellite-to-ground links in particular, the impact of atmospheric turbulence on the signal propagation requires an optimization of the coupling of light in single-mode optical fibers (SMF), necessary to interfacing with ground stations.

In this paper, we focus on the impact of free-space propagation on the link feasibility and performance in terms of secret key rate, assuming a single-mode detection of the quantum signal on the ground. For the first time, we use a refined modeling of SMF coupling statistics accounting for both satellite pointing jitter and atmospheric turbulence residual impact after a close-loop correction performed by adaptive optics (AO). We use realistic configurations of prepare-and-measure QKD, with both discrete and continuous variable encodings, and including finite size effects, and carefully select the atmospheric turbulence parameters to obtain representative observing conditions.

Our baseline scenario is a single downlink QKD connection. Alice is located in a Low Earth Orbit (LEO) satellite which sends a 1550 nm beam with a divergence of 10 μrad and whose pointing error has a standard deviation of 1 μrad. Bob is in the ground station with a 1.5 m diameter telescope followed by an AO correction system [12].

2. Propagation channel model

If in free-space, signal attenuation increases quadratically with propagation distance, it also involves new challenges, such as : beam wandering, limited time window of satellite visibility, atmospheric turbulence-induced wavefront perturbation. The latter significantly hinders the coupling into a SMF.

To model the atmospheric channel we exploited thousands of measurements taken at astronomical sites from three different databases [13–15] in order to construct statistically significant daytime and nighttime turbulence profiles. These profiles consist of a series of C_n^2 values, each describing the distribution of the turbulence strength along a line of sight for a specific turbulence scenario and a particular elevation. Each profile can also be characterized by integrated parameters such as the Fried parameter r_0 which characterizes the turbulence strength integrated along the line of sight and the isoplanatic angle θ_0 which characterizes the angular evolution of the wavefront as well as its temporal evolution in the case of LEO slewing satellites. We have chosen baseline day and night profiles which correspond to r_0 and θ_0 values on the lower quartiles of probability of the measurements available in the databases, some of the day profiles can be observed in Figure 1a.

3. Adaptive Optics model

The AO system consists of a feedback loop with a wavefront sensor that measures the aberrations of the disturbed beam, a multiple actuator deformable mirror that corrects part of these aberrations, and a real-time computer driving the real time close-loop system. AO therefore provides partial real-time correction of the turbulence hence

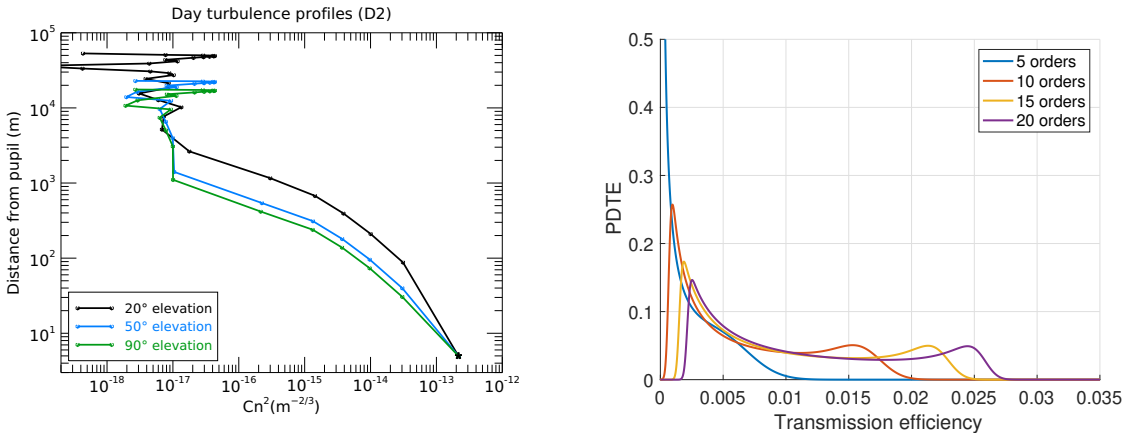

(a) (b)

Fig. 1: (a) Baseline daytime profiles at different elevations. At zenith, r_0 = 10.6 cm and θ_0 = 25.8 μrad. (b) Probability distribution of the transmission for a 500 km satellite for different levels of AO correction.

improving the SMF coupling and the overall optical channel leading to a better recovery of the quantum signal and ultimately an increase on the key rate.

To model the AO correction, we use the pseudo-analytical simulation tool SAOST [16], which employs a Monte-Carlo type simulation to produce multiple random occurrences of complex amplitude for a particular combination of satellite orbit, turbulence profile and given AO system parameters. SAOST modeling accounts for aperture averaged amplitude fluctuations, so-called scintillation, and provides an accurate modeling of the turbulent phase AO partial correction. This AO modeling accounts for the limited wavefront sensor spatial sampling (aliasing), the limited number of correction modes (fitting) and the loop limited temporal sampling (temporal error). In parallel, the effects of beam wander due to satellite pointing error are determined by using the model proposed by [17]. After running both simulations for different elevations along the trajectory of the satellite, they are combined and the statistical representation of the transmission efficiency is derived, as illustrated in Figure 1b for different levels of AO correction. For each one of the occurrences the residual error is calculated and we then compute its complex coupling with the fiber mode via an overlap integral which results in a value of coupling efficiency. With enough iterations performed we can derive a probability distribution of the coupling efficiency.

We consider an AO system with a 2-frame delay loop with integral controller running at a 5 kHz sampling frequency and we consider the correction of 1, 5, 10, 15 or 20 Zernike radial orders. For a 15 radial order correction (136 modes) we obtain at zenith an overall wavefront error of 0.48 rad², bringing a huge gain compared to the uncorrected variance (about 85 rad²). The AO corrected variance is distributed, respectively on aliasing, fitting and temporal error, as follows: 0.09 ; 0.28 ; 0.11 rad². As expected, with a fast loop, the error is dominated by spatial terms (aliasing and fitting) hence the emphasis in our study on the impact of the number of corrected modes on key rate performance.

4. Secret key rate

In this particular study we have chosen to consider the decoy-state efficient BB84 DV-QKD protocol and a Gaussian modulation of amplitude and phase CV-QKD protocol. The key generation rate is first computed for an asymptotic regime and then taking into account finite-size effects which are particularly important in this scenario due to the limited communication time with the satellite. These effects are accounted for by taking the worst case scenario of the parameters for a given number of symbols exchanged. The simulations were done for different noise levels as well. For CV, typical values of excess noise ξ of 0.01, 0.03 and 0.05 SNU were used. For DV, a pessimistic Y_0 =8.1e-5 high noise scenario was computed from the background photon rate measured in a passage of the GLONASS satellites with the solar panels reflecting solar radiation into the receiver. A more optimistic background noise value for daytime of Y_0 = 2.1e-5 was calculated from the LOWTRAN [18] sky radiance for a rural environment with 23 km visibility. For nighttime, background sky noise can be neglected and the yield was calculated from the detector dark counts as Y_0 = 1e-7.
In Figure 2, we present some of the results we obtained in this study. The graphs on the upper section show the estimated key rate for a range of altitudes corresponding to LEO satellites, under moderate turbulence conditions and assuming a simple tip-tilt correction, the minimum correction required for tracking purposes. The graphs on the lower section meanwhile, show the result of employing a higher order correction with a more complex AO system. We can observe that with the sole tip-tilt correction, it is only possible to obtain a key in the asymptotic regime (i.e. when assuming an infinitely long transmission) and not in a more realistic finite-size case.

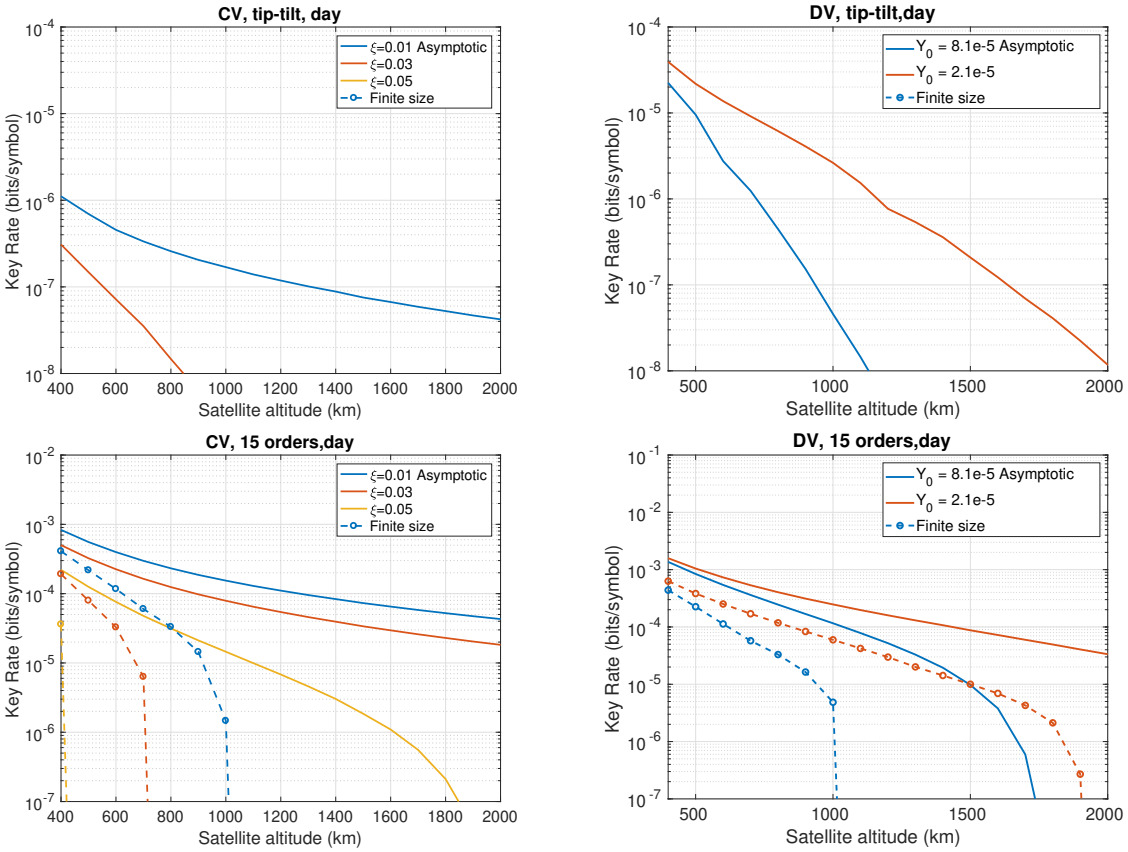

Fig. 2: Secret key rate for the CV (left) and DV (right) protocols in daytime for tip-tilt (top) and 15 order (bottom) AO correction. The colors represent different levels of excess noise ξ for CV and background noise Y_0 for DV. Represented in dashed lines are the finite-size simulations.

5. Conclusion

The use of adaptive optics with high order correction (here 15 radial orders that is 136 modes) allows for the establishment of keys, even when considering finite size effects and for the most severe noise cases considered in both protocols. Through the improvement of the efficiency of the channel, AO also permits higher key rates, with improvements of around one and three orders of magnitude in DV and CV, respectively. Additional results obtained in other conditions and a more detailed description of our simulation process and analysis can be found in [12]. Our results prove that adaptive optics is mandatory for satellite-to-ground QKD with single mode detection. We are currently working on an in-lab experimental validation with emulation of the AO corrected atmospheric channel.

References

1. J.-P. Chen, C. Zhang, Y. Liu, et al., Phys. Rev. Lett. 124, 070501 (2020).
2. J.-P. Chen, C. Zhang, Y. Liu, et al., Nat. Photon. 15, 570 (2021).
3. M. Pittaluga, M. Minder, M. Lucamarini, et al., Nat. Photon. 15, 530 (2021).
4. S.-K. Liao, W.-Q. Cai, J. Handsteiner, et al., Phys. Rev. Lett. 120, 030501 (2018).
5. D. Y. Vasylyev, A. A. Semenov, and W. Vogel, Phys. Rev. Lett. 108, 220501 (2012).
6. S. Pirandola, U. L. Andersen, L. Banchi, et al., Advances in Optics and Photonics 12, 1012 (2020).
7. S.-Y. Shen, M.-W. Dai, X.-T. Zheng, et al., Phys. Rev. A 100, 012325 (2019).
8. C. Liorni, H. Kampermann, and D. Bruss, New J. Phys. 21, 093055 (2019).
9. M. Polnik, L. Mazzarella, M. D. Carlo, et al., EPJ Quantum Technol. 7, 3 (2020).
10. D. Dequal, L. Trigo Vidarte, V. Roman Rodriguez, et al., npj Quantum Information 7, 3 (2021).
11. S. Ecker, B. Liu, J. Handsteiner, et al., npj Quantum Information 7, 5 (2021).
12. V. Marulanda Acosta, D. Dequal, M. Schiavon, et al., https://arxiv.org/abs/2111.06747 (2021)
13. D. Sprung, et al., Proc. SPIE 8890, 889015 (2013)
14. J. Osborn, et al., MNRAS, Vol 478-1, (2018)
15. H. Vázquez Ramió et al., PASP 124 868, (2012)
16. N. Védrenne et al., Proc. SPIE 9739, (2016)
17. D. Yu. Vasylyev et al., PRL 108, 220501, (2012)
18. F. X. Kneizys, E. P. Shettle, L. W. Abreu, et al., Air Force Geophysics Laboratory (1988).